

~~Electrical conductivity measurements as a proxy for diffusion-limited microbial activity in soils~~
Electrical conductivity measurements as proxies for diffusion-limited microbial activity in soils under controlled laboratory conditions.

5 Orsolya Fülöp^{1,2}, Naoise Nunan^{2,3}, Mamadou Gueye², Damien Jougnot¹

¹ Sorbonne Université, CNRS, EPHE, UMR 7619 METIS, F-75005 Paris, France

² Sorbonne Université, CNRS, IRD, INRAE, UPEC, Institute of Ecology and Environmental Sciences – Paris, F-75005 Paris, France

³ Department of Soil and Environment, Swedish University of Agricultural Sciences, Uppsala, Sweden

10

Correspondence to: Naoise Nunan (naoise.nunan@cnrs.fr)

Short summary:

Soil microorganisms exist in a highly structured ~~and variably connected environment, in which, variably connected~~ environment, where they play a critical role in organic matter dynamics. To investigate the relationship between soil respiration and the connectivity of the soil pore water phase, we ~~analysed~~ studied the use of electrical conductivity as a proxy for soil respiration. ~~Our results show that there were non-linear relationships between the two variables, thereby opening up a new approach to better understand soil respiration.~~ Our results show that there were non-linear relationships between the two variables, thereby opening up a new approach to better understand soil respiration.

Abstract:

Soils play a dynamic role in the carbon cycle, functioning as both a source and a sink for atmospheric carbon. Despite their importance, uncertainties in soil-atmosphere interactions persist due to the complex processes governing soil carbon dynamics. Microbial access to substrate is a key mechanism regulating organic C decomposition. Evidence suggests this access is diffusion-limited, as reflected in the strong dependence of soil respiration on water availability. In recent years, non-destructive geophysical tools, including electrical conductivity measurements, have been used to determine the water content of soils and the connectedness of the water phase in the soil pore network. As both respiration and electrical conductivity may depend on water availability and connectivity, our study aimed to determine whether electrical conductivity measurements could serve as a proxy for soil respiration when microbial activity is potentially diffusion-limited. This was done by measuring electrical conductivity and respiration rates at different matric potentials, using sieved and undisturbed top- and subsoil samples taken from conventional tillage and conservation agriculture management plots of a Luvisol. Soils play a highly dynamic role in the carbon cycle, by acting as either a carbon source or sink for atmospheric carbon. Despite their importance in the global carbon cycle, uncertainties surrounding soil-atmosphere interactions remain, due to the many mechanism processes that underlie soil carbon dynamics. One of the main mechanisms determining the decomposition of organic C in soil is the access microbial decomposers have organic substrate to to substrates. Esuggestsmay beEWhile not yet formally tested, there is evidence to support the idea that microbial decomposer access to substrates is diffusion limited. This is underlined by soil respiration rates being strongly dependent on water availability. In recent years, non-destructive geophysical tools, including electrical conductivity measurements, have been used to determine the water content of soils and the connectedness of the water phase in the soil pore network. As both respiration and electrical conductivity may depend on water availability and connectivity, our study aimed to determine whether electrical conductivity measurements could be used as a proxy of soil respiration when diffusion limited microbial activity is potentially diffusion limitedn soils. This was done by measuring electrical conductivity and respiration rates at different matric potentials using. Ssieved and undisturbed top and subsoil samples taken from conventional tillage and conservation agriculture management plots were used. Our results revealed an initial increase followed by a subsequent decrease in soil respiration with increasing matric suction (i.e., decreasing water saturation). Our results revealed an initial increase and consecutive drop in soil respiration associated with a decrease in the matric potential. The

Mis en forme : Justifié, Interligne : 1,5 ligne

Electrical conductivity followed a similar decrease throughout the experimental range and these showed a significant non-linear decreased across the experimental range as the soil desaturated. The two variables, and the data exhibited a significant nonlinear relationship, indicating a shared sensitivity to changes in aqueous phase connectivity. Finally, we propose a quantitative approach for estimating the evolution of the water tortuosity of the water phase in the samples, based on the from electrical conductivity measurements, was used to and show a clear relationship between water phase tortuosity and with respiration measurements. These results thus suggest that both measured variables depend on the connectedness of the aqueous phase and highlight the potential of electrical conductivity measurements as a mechanistically informed proxy for diffusion-constrained soil respiration, suggest that they could be used as groundwork for further investigations into soil respiration and electrical conductivity dynamics.

50

55

Keywords: Soil respiration, Microbial activity, Carbon cycle, Diffusion limitation, Water availability, Electrical conductivity, Pore connectivity, Soil moisture, [Geophysical measurements](#) [Tortuosity](#)

1. Introduction

60

~~Natural soils contain the most diverse terrestrial microbial communities as well as terrestrial organic carbon reserves with quantities surpassing those found in both the atmosphere and vegetation combined. Natural soils contain the most diverse terrestrial microbial communities as well as terrestrial organic carbon reserves with quantities surpassing that found in both the atmosphere and vegetation combined.~~ (Crowther et al., 2019; Dubey et al., 2020). ~~They are part of a highly dynamic cycle associated with a balance between soils acting as a carbon sink or source for atmospheric carbon.~~ Through microbial processing of organic inputs, soils function either as a carbon sink or a source, depending on the balance between carbon inputs and losses (Hargreaves et al., 2015; Six et al., 2006). Carbon (C) inputs ~~to soil~~ are processed by microbial communities and are either released to the atmosphere ~~(generally in the form of as CO₂)~~ or are converted into microbial biomass and ultimately soil organic matter (Al-Maliki & Ebreesum, 2020; Fan et al., 2015; Sandor et al., 2020). ~~Several~~ A number of factors ~~are believed to~~ modulate soil C dynamics~~the dynamics of C in soil~~, including the intrinsic resistance of ~~the~~ organic molecules to decomposition, the spatial inaccessibility of organic matter (OM) to microbial decomposers, and organo-mineral associations (Lützow et al., 2006). ~~Because decomposition occurs when organic molecules encounter microbial decomposers or their extracellular enzymes. As~~ The decomposition of OM occurs when organic molecules encounter microbial decomposers or their extracellular enzymes. (Dignac et al., 2017). ~~the spatial separation of OM and decomposers is also believed~~ considered ~~to be a major constraint on decomposition, in soils as~~ microorganisms and OM are heterogeneously distributed and occupy only a small fraction of the soil pore system ~~as both microorganisms and OM are heterogeneously distributed, and only cover a small percentage of the soil pore system.~~ (Dignac et al., 2017; Lützow et al., 2006). Thus, decomposition requires the movement of substrates, microorganisms, or both. This means that for decomposition to occur, one or the other, or both, must move.

80

A relatively small proportion of ~~the~~ soil microbial communities possesses the capacity for flagellar motility, primarily in ~~most of which is limited to~~ zones with high OM contents (Ramoneda et al., 2024), such as the rhizosphere. ~~This means that microbial~~ Microbial decomposition of OM therefore largely relies on the diffusion of organic molecules toward decomposers ~~may rely on the diffusion of organic molecules towards decomposers~~ (Nunan et al., 2020). ~~Diffusion limitation is supported by observations that OM decomposition often varies linearly with the square root of time, a characteristic of diffusion-controlled processes. The diffusion limitation of OM decomposition is supported by the observation that it often varies as a linear function of the square root of time (Stanford & Smith, 1972), a characteristic of diffusion limited processes. Because substrate diffusion occurs only in the presence of water, partially saturated soils require continuity of the aqueous phase across connected pores. As substrate diffusion can only occur in the presence of water, in the context of partially saturated soils, this would correspond to the necessity of the aqueous phase reaching across connected pores (Lang et al., 2007). Respiration declines sharply at low water contents.~~ This reliance on the presence of water is underlined by studies indicating respiration

90

becoming virtually undetectable at very low water contents (Davidson et al., 1998), highlighting the central role of water availability in regulating microbial activity. The availability of water has been identified as the single most important factor affecting microbial processes, including microbial respiration (Kpemoua et al., 2023; Nasiri et al., 2023). However, the mechanistic hierarchy underlying this relationship remains unclear. Although the relationship between moisture levels and carbon decomposition is well established, the hierarchy of mechanisms underlying the relationship is not certain. In partially saturated soils, diffusion limitation arises not only from reduced water content but also from loss of continuity in the water-filled pore network, which increases tortuosity and constrains substrate diffusion through the aqueous phase (Ghanbarian et al., 2013; Ebrahimi & Or, 2015; Ghezzehei et al., 2019). (Jougnot et al., 2009; Revil & Jougnot, 2008).

Geophysical methods are increasingly applied as fast, non-destructive approaches to monitor soil moisture dynamics (Garre et al., 2021; Hermans et al., 2023; Loiseau et al., 2023) and to infer water-phase connectivity in porous media (Ghanbarian et al., 2013; Li et al., 2015; Jougnot et al., 2018; Wilson et al., 2024). Electrical conductivity (EC) measurements are particularly sensitive to connectivity within the aqueous phase, through which charge carriers move, enabling characterization of pore spaces supporting solute diffusion (Jougnot et al., 2009; Revil & Jougnot, 2008). When measured across a range of soil matric potentials (i.e., water contents), EC responds to changes in aqueous phase continuity and tortuosity that control diffusive transport. Accordingly, EC is widely used to monitor spatial and temporal variations in the connectivity of the water-filled pore space. Geophysical tools are fast and cost-effective tools for the measurement of soil moisture contents and also provide insight into the spatial characterization of porous material (e.g., Garre et al., 2021; Hermans et al., 2023; Loiseau et al., 2023). Electrical conductivity measurements are particularly sensitive to the connectivity of the conductive phase; that is the aqueous phase, where charge carriers move thereby enabling the characterization of pore spaces in which solute diffusion takes place (Jougnot et al., 2009; Revil & Jougnot, 2008). (Garre et al., 2021; Hermans et al., 2023; Loiseau et al., 2023).

With both respiration and electrical conductivity potentially relying on the diffusion of either substrates or charge carriers across soil systems, this raises the question of whether electrical conductivity measurements could act as a proxy for soil respiration in the absence of water flow. Different soil matric potentials correspond to different water contents, which alter pore connectivity and tortuosity and therefore influence diffusion-controlled transport processes (Revil and Jougnot, 2008; Ghanbarian et al., 2013; Jougnot et al., 2018).

To address this question and improve our understanding of the relationship between microbial respiration and diffusion, this study aimed to investigate the relationship between soil respiration and electrical conductivity across a range of soil matric potentials. This relationship was examined to evaluate a novel methodology for the rapid characterization of soil biological processes. Measurements were conducted on both sieved and undisturbed topsoil and subsoil samples from two treatments of a long-term field trial.

Code de champ modifié

Mis en forme : Français (France)

Mis en forme : Français (France)

Code de champ modifié

Mis en forme : Français (France)

Mis en forme : Français (France)

Mis en forme : Taquets de tabulation : 3,56 cm,Gauche

Mis en forme : Anglais (États-Unis)

Mis en forme : Anglais (États-Unis)

125 Our primary hypothesis was that under diffusion-limited conditions, microbial respiration rates are positively correlated with
electrical conductivity due to their shared dependence on diffusive transport. We further hypothesized that higher initial carbon
availability would weaken this relationship, as a broader distribution of organic substrates reduces diffusion constraints. In this
context, we expected differences between topsoil and subsoil samples to emerge. Finally, we hypothesized that sieving
homogenizes the pore network, resulting in more consistent relationships between electrical conductivity and respiration than
130 those observed in undisturbed soil samples.

-Consequently, these techniques are increasingly used to monitor the spatial and temporal distribution of water-filled pores in
soils (Friedman, 2005; Jougnot et al., 2018; Samouëlian et al., 2005):

135 ~~processes pore space~~As both respiration and electrical conductivity depend, respectively, on the diffusion of substrates or
charge carriers through soil pore space, electrical conductivity measurements might serve as a proxy for soil respiration when
water flow is negligible. ~~Different soil matric potentials correspond to different water contents, which alter pore
connectivity and tortuosity and therefore influence diffusion-controlled transport processes (Ghanbarian et al., 2013;
Jougnot et al., 2018), assess the possibility of developing a microbial respiration in the water phase would result,
due to the homogenisation of the pore network~~With both respiration and electrical conductivity potentially relying on
140 the diffusion of either substrates or charge carriers across the soil systems, this raises the question of whether electrical
conductivity measurements could act as a proxy for soil the quantification of soil respiration in the absence of water
flow. To answer this question and improve our understanding of the relationship between microbial respiration and
diffusion, our study first of all aimed to investigate the relationship between soil respiration and electrical conductivity
at different soil matric potentials. The measurements were conducted on both sieved and undisturbed top- and subsoil
145 samples taken from two different treatments of a long-term field trial.

Our primary hypothesis was that in diffusion-limited conditions, microbial respiration rates will be positively correlated with
electrical conductivity stemming from a shared dependence on diffusive transport. We further hypothesized that higher initial
carbon availability would weaken this correlation, due to the broader distribution of organic substrates reducing diffusion
constraints. In the case of our samples we believe this would cause differences between topsoil and subsoil samples to emerge.
150 Finally, we hypothesized that sieving would homogenize the pore network, resulting in more consistent relationships between
conductivity and respiration compared to those observed in undisturbed soil samples.

2. Material and Methods

2.1. Study site and sample collection

The soil used in the study was collected from the “La Cage” field experiment on the French National Institute for Agricultural
155 Research (INRAE) campus in Versailles, Ile-de-France (48°45'N; 2°08'E). ~~When looking at t~~The climate of the greater
Parisian basin climate, it is characterized as being under temperate climate. The climate in the greater Parisian basin can be
characterised as temperate, with an average precipitation of 630 mm and an annual average temperature of 10.4 °C (Bellone
et al., 2023). The soil is a well-drained Luvisol (Autret et al., 2020). The experimental site was established in 1998 to conduct

Mis en forme : Couleur de police : Texte 1

160 long-term field studies on the effects of different cultivation methods on a well-drained Luvisol soil (Autret et al., 2020). We
~~decided to test two types of soils coming from two different fields. Soil from two treatments, conventional tillage and one
being the other conservation agriculture treatment trial fields, were tested. This study focused on the conventional tillage and
conservation agriculture fields.~~ The conventional tillage site underwent annual ploughing to a depth of 30 cm and systematic
pesticide application. In contrast, the conservation agriculture ~~treatment site~~ was not tilled and was maintained with persistent
cover crops. ~~For the conservation agriculture site, pesticides were applied only when plant damage was detected in the
conservation agriculture treatment. Pesticides were only applied in the conservation agriculture site if plant damage was
observed.~~

170 ~~Both fields were under plant cover at the time of sampling. Since sampling occurred during the off-season in early
November 2023, between the main crop. This coverage corresponded to e-plant cover of the conventional tillage field was
mustard in the case of the conventional tillage field, and common vetch and black oats for the conservation agriculture field
while that of the conservation agriculture was common vetch and black oats. These were in place to protect the soil.~~ The main
crops consisted of a wheat-pea-rapeseed crop rotation for the conventional tillage site and pea-wheat-corn-oat rotation for the
conservation tillage site. A more detailed description of the plant cover ~~and management practices is provided in used and
field treatment practices can be found in~~ Autret et al. (2016). The choice to use ~~the conventional tillage and conservation
agriculture treatments was based upon the fact that these were likely to~~ the conventional tillage and conservation agriculture
175 ~~treatments was based on the expectation that these would~~ have different soil structures and C contents, both key factors
influencing carbon dynamics. ~~The selection of these two systems is supported by findings from the La Cage study, which show
that conservation agriculture generally sustains higher microbial biomass, total C, and significantly greater stabilized soil
organic carbon content compared to conventional tillage. The selection of these two systems is supported by findings from the
LaCage study site, which show that conservation agriculture generally sustains higher microbial biomass, total C and
significantly greater bound organic carbon content compared to conventional tillage (Henneron et al., 2015; Juarez et al., 2013).~~
180 Further studies have identified the presence of more stable ~~water-soluble~~ water-soluble aggregates and associated improved
porosity in the conservation agriculture fields compared to conventional tillage treatments (Chabert & Sarthou, 2020;
Cosentino et al., 2006). ~~This~~ This improved aggregate stability is ~~expected to influence~~ believed to impact the maintenance of
185 pore connectedness across a range of matric potentials (Mondal & Chakraborty, 2022).

~~To obtain~~ In order to have a wide range of pore size distributions, pore connectivity, carbon contents and microbial biomass,
we used sieved (<2 mm) and undisturbed samples from the topsoil (0–15 cm) and subsoil (50 cm). The soil microbial biomass
and soil C contents are known to decrease with depth ~~of down~~ the soil profile (Salomé et al., 2010) and sieving changes the
190 physical structure and water retention properties of soil (Herbst et al., 2016).

~~The undisturbed samples were collected by inserting PVC sampling cores (80 mm in length and 58 mm in internal diameter)
directly into the soil horizons and Undisturbed samples were obtained by inserting PVC sampling cores (80 mm in length and~~

195 ~~58 mm in internal diameter) directly into the soil horizons and extracting them carefully to preserve the~~ carefully extracting them to preserve soil structure. All undisturbed samples were frozen at -20°C until use to minimize organic matter decomposition during storage prior to incubation experiments. ~~This was done to minimize organic matter decomposition that might occur during the preservation of samples prior to the incubation experiments.~~ (Allende-Montalbán et al., 2024). Bulk soil collected ~~for sieving to prepare sieved samples~~ was air-dried, sieved to 2 mm, and stored at 10°C until the experiment began.

2.2 Sample preparation for incubation

200 Undisturbed samples were thawed gradually by transferring them from a deep freezer to an 8 °C refrigerator for 24 hours, followed by five days at 20 °C in the laboratory prior to incubation. Sieved samples were prepared by packing soil to a target bulk density of 1.73 g cm⁻³, corresponding to the average bulk density measured in undisturbed samples. Because the undisturbed cores were collected under very wet field conditions, some disturbance during sampling may have affected the measured bulk density. This bulk density value was therefore used only to obtain comparable soil mass and pore volume between treatments and not to reproduce the in situ soil structure.

Samples were saturated by capillary rise by initially placing them in 1 cm of water, with additional water added gradually over 24 hours until full saturation was achieved. The samples were then transferred to airtight microcosms and incubated in the dark to limit algal growth on the microcosm surface caused by light exposure.

2.3.2. Study approach and incubation set-up

210 This study examined the effect of soil water status on respiration rates and electrical conductivity during short-term incubations. To impose different soil water contents without physically disturbing the samples, matric potentials of -70, -100, -250, -350, -450 and -630 hPa were applied using a suction system. The corresponding conversion between matric potentials and water content is described in Section 2.4.3.

215 Samples were placed in airtight microcosms fitted with a ceramic plate allowing adjustment of the pressure head and a septum for headspace sampling ~~(the microcosms used by The study analysed the effect of matric potential, corresponding to different crop available soil water contents, on soil respiration rates and electrical conductivity during short term incubations of samples at varying pressure heads (-70, -100, -250, -350, -450 and -630 hPa). Samples were placed in airtight microcosms fitted with a ceramic plate, allowing for adjustments of the pressure head, and a septum for headspace sampling (Poll et al., 2010; Fig.1)).~~ The ceramic plate positioned at the base of each microcosm was connected to a suction pump, enabling precise pressure-head control of the soil cores. Additionally, an opening in the lid was used to route electrical cables for conductivity measurements. A schematic of the setup is provided in Fig. S1.

Mis en forme : Normal

Mis en forme : Couleur de police : Texte 1

225 Five microcosms at a time were subjected to controlled suction, and drained water was collected in refrigerated bottles at 4 °C for subsequent analysis of soil solution ionic strength. One microcosm was used exclusively for gravimetric measurements to verify changes in moisture content. Each treatment was performed in triplicate. A, which had a pump to
230 Incubations were conducted at 20 °C. Samples were maintained at each pressure head for approximately 24 hours after leaching had ceased to allow hydraulic equilibrium to be reached. In total, 24 microcosms were used (four soils × two structural treatments × three replicates). Samples were analysed in randomized order such that replicates from the same soil and treatment combination were not measured simultaneously.

~~Incubations were conducted at 20°C. Samples were maintained at each pressure head for approximately 24 hours after leaching had ceased to allow hydraulic equilibrium to be reached. In total, 24 microcosms were used in the experiment, corresponding to four soils, two structural treatments, and three replicates. Samples were analysed in a randomized order, such that replicates from the same soil and treatment combination were not measured simultaneously. Five microcosms at a time were subjected to controlled suction using a pump, and the drained water was collected in refrigerated bottles at 4°C for subsequent analyses of the ionic strength of the soil solution across matric potentials. One of the microcosms was exclusively used to weigh samples in order to ensure that changes in moisture content were as expected. Each treatment was carried out in triplicate. A schematic description of the laboratory set-up can be found in Fig. S1 of the supplementary materials. The incubations were carried out at 20°C. The samples were held at each pressure head for approximately 24 hours after no more water leaching was observed to achieve hydraulic equilibrium. In total there were 24 microcosms (4 soils x 2 structural treatments x 3 replicates) used during the experiment. The samples were analysed in a randomized fashion, i.e. no replicates from the same sample and treatment combination were measured at the same time.~~

245 ~~After the measurements at -630 hPa were completed, samples were transferred to mason jars fitted with septa for headspace sampling and containing an oversaturated lithium chloride solution. This induced a suction at the sample surface corresponding to a pressure head of -996 hPa. After measurements at -630 hPa were completed, samples were transferred to mason jars equipped with a septum to allow headspace sampling and containing an oversaturated lithium chloride solution. This induced a suction at the sample surface that is equivalent to a pressure head of -996 hPa (Colas, 2011.; Greenspan, 1977). Sample weights were monitored periodically until no further mass loss was observed, indicating that the target pressure head had been reached. Sample weights were monitored periodically to determine whether the target pressure head had been reached, with measurements continuing until no further water loss was observed.~~

Mis en forme : Police :10 pt, Couleur de police : Texte 1

Mis en forme : Avec coupure mots

2.3 Sample preparation for incubation

255 Undisturbed samples were thawed gradually by transferring them from a deep freezer to an 8°C refrigerator for 24 hours, then
to a 20°C laboratory for five days prior to the beginning of the incubations. Sieved samples were prepared by packing the soil
to a bulk density of 1.73 g/cm³, equivalent to the average density of undisturbed samples. Samples were saturated via capillary
rise by initially placing them in 1 cm. Water was added gradually over the course of 24 hours until full saturation of the soil
samples was achieved. The samples were then transferred into airtight, sealed microcosms and incubated in the dark, in order
260 to reduce algal growth on the surface of the microcosms that could be caused by direct sunlight.

2.4 Analytical data collection

2.4.1 CO₂ flux measurements

Soil respiration rates were measured by taking four gas samples (20 mL each) from the microcosm headspace at each applied
matrix potential. CO₂ concentrations were analysed using a micro gas chromatograph (micro-GC, Agilent 3000). The
265 instrument was equipped with a PLOT Q column (Poropak Q) to separate CO₂ from other gases, and helium was used as the
carrier gas. Detection was performed with a thermal conductivity detector (TCD). Respiration rates were calculated from the
increase in CO₂ concentration over time. Additional details of the microcosm and gas sampling setup are shown in Fig. S1.
For the characterization of the soil respiration flux, the slope of CO₂ accumulation over time was determined by linear
regression (R base stats package) and visualized using ggplot2 (v. 4.0.1). Specifically, the respiration flux (F_{CO_2}) was obtained
270 as the slope of the linear regression of CO₂ concentration (C , ppm) against time (t , s):

$$F_{CO_2} = \frac{dC}{dt} \quad (1)$$

The flux per gram of organic matter (F_{OM}) was then calculated as,

$$F_{OM} = \frac{F_{CO_2}}{m_{OM}} \quad (2)$$

where m_{OM} is the organic matter mass (g) in each sample.

275 For the visualization of the soil respiration rate, we used the relative soil respiration (F_{rel}) as the ratio of the flux at the given
condition to the flux at -70 hPa.

$$F_{rel} = \frac{F_{OM}}{F_{OM(-70hPa)}} \quad (3)$$

The -70 hPa condition was used as the reference, corresponding to the highest water content treatment.

280 Soil respiration rates were determined by measuring the increase in CO₂ concentration in the microcosm headspace three times
over a period of 48 to 72 hours, depending on the rate at which CO₂ accumulated, by gas chromatography (Agilent 3000).

2.4.2 Electrical Conductivity Measurements

Sample electrical conductivity was monitored using a PSIP unit (Portable Spectral Induced Polarisation, Ontash and Ermac;
ontash.com) in parallel with soil respiration measurements. The PSIP unit was fitted to a custom-made electrode configuration

Mis en forme : Normal

Mis en forme : Normal

285 for each sample. A voltage of 5 V was imposed between the current injection electrodes, and the real part of the complex
conductivity at 1 Hz was recorded and averaged over five periods. A frequency of 1 Hz was used, as this is the most commonly
employed frequency for electrical conductivity measurements in field studies. Sample electrical conductivity was monitored
using a PSIP unit (Portable Spectral Induced Polarisation by Ontash and Ermac, ontash.com) in parallel with soil respiration
measurements. The PSIP unit was fitted to a custom-made electrode configuration on each sample. A frequency of 1 Hz was
used, aligning with the most commonly employed frequency when measuring in electrical conductivity for field studies (e.g.,
290 Blanchy et al., 2025).

The PVC cores were fitted with brass screws, 1.5 mm in diameter and 16 mm in length, which served as electrodes. The
electrode configuration and corresponding geometrical factors were determined using COMSOL Multiphysics 5.0 and are
shown in the Supplementary Material (Fig. S2). Each electrode was inserted 6 mm into the soil cores to ensure consistent soil
295 contact and to minimize the effects of minor shrinkage caused by moisture loss at the sample edges.
Injection electrodes were positioned at the top and bottom of the samples, while three pairs of potential electrodes were inserted
vertically and one pair horizontally to capture a broader distribution of current lines within the sample. Electrical conductivity
was calculated using the geometrical factors listed in Table S1 of the Supplementary Material.
For the electrical conductivity analysis, the estimated soil water content saturation (S_w) was used for each sample. Bulk
300 electrical conductivity was fitted using the following pedophysical relationship (Waxman & Smits, 1968),

$$\sigma = \frac{S_w^n}{F} (\sigma_w + \frac{\sigma_s}{S_w}), \quad (4)$$

where S_w is water saturation (-), F the formation factor (-), n the saturation exponent (-), σ_w the pore water conductivity (S/m),
and σ_s the surface conductivity (S/m). Model parameters were estimated using nonlinear least squares fitting.
This fitting procedure also allowed the estimation of tortuosity, τ_w (-), as a function of water saturation following Jougnot et
305 al. (2018),

$$\tau_w = \Phi F S_w^{(1-n)}, \quad (5)$$

where Φ is the sample porosity (-) derived from bulk density measurements as described in Section 2.4.3.

The PVC cores were equipped with brass screws (1.5 mm thick and 16 mm long), which served as electrodes. The electrode
configuration and corresponding geometrical factors were determined using COMSOL Multiphysics 5.0 software and can be
found represented in the Supplementary materials (Fig. S2). Each electrode was inserted 6 mm into the soil cores to ensure
310 reproducibility by maintaining optimal soil contact and avoiding minor shrinkage effects caused by moisture loss around the
sample edges. The injection electrodes were positioned at the top and bottom of the samples respectively, with three pairs
inserted vertically and one pair inserted horizontally to capture a broader distribution of electrical lines throughout the sample.
Electrical conductivity values were calculated using the geometric factors outlined in Table S1 of the supplementary materials.

Mis en forme : Police :Italique

Mis en forme : Indice

2.4.3. Organic matter and water content retention measurements data collection

After the incubation measurements, the samples were dried at 105 °C for 24 hours to obtain the final water content of each sample. After the measurements had been concluded, the samples were dried at 105°C for 24 hours to obtain the final water content of each sample. A subsample was then ground in order to measure total organic matter content by loss-on-ignition.

320 For this step, we followed the procedure outlined in Hogsteen et al. (2015) whereby Hogsteen et al. (2015), in which samples were heated at 550°C for 3 hours in a Nabertherm oven.

325 Independent samples were collected to determine water retention curves using a Richards's pressure plate apparatus. Samples were subjected to pressure heads ranging from 0 to 15,000 hPa, and corresponding changes in mass were recorded to calculate water content at each pressure step. Water retention data were fitted using the van Genuchten model (Van Genuchten, 1980) implemented in the soilphysics package (v. 5.0) in R (R Core Team, 2023). Model parameters (α and n) were estimated separately for each soil and structural treatment. The fitted retention functions were subsequently used to convert the applied pressure heads during the incubation experiment into corresponding volumetric water contents for each sample. The fitted water retention curves for all soil and structural treatments are provided in Fig. S4 of the Supplementary Material. ~~Were~~ carried out (Van Genuchten, 1980)

330

2.4.4. Statistical analysis and data visualisation

2.4.4. Statistical analysis and data visualisation

The statistical analysis and data visualization were conducted using RStudio (v. 4.3.0; R Core Team, 2023). (Waxman & Smits, 1968) Overall variance across sampling sites and depths was tested using Type III ANOVA with Welch's correction and Satterthwaite's method for degrees of freedom, implemented via the ggstatsplot package to account for unbalanced data.

335

Finally, soil respiration rate was plotted as a function of sample tortuosity. Regression analyses were performed using linear mixed-effects models fitted with the nlme package to assess differences among sampling depths and field treatments.

340

(1) (2) (3) (Waxman and Smits, 1968) (4) () () () (S/m) (S/m), (), evolution as a function of the water saturation (Jougnot et al., (2018))

Mis en forme : Titre 3

Mis en forme : Gauche, Interligne : simple, Avec coupure mots

Mis en forme : Surlignage

Mis en forme : Surlignage

Mis en forme : Droite

345 where θ is the sample porosity (θ). The statistical analysis was conducted in RStudio (v. 4.3.0; R Core Team 2023). The respiration flux was obtained by determining the slope of the regression plots of CO₂ accumulation against time. The CO₂ flux per gram of organic matter equivalent per hour was then used to calculate the CO₂ flux relative to the flux at -70 hPa.

350 Comparison between the relative fluxes and electrical conductivity measurements of each sample across the matric potential range was made using a linear mixed-effect model (fit using the nlme package) to determine differences among depths and field treatments.

355 Variance across matric potentials was assessed, and pairwise differences were tested using Type III ANOVA with Satterthwaite's method for degrees of freedom, implemented via the "ggstatsplot" package, to account for unbalanced data. The electrical conductivity data was represented as a relative conductivity compared to the highest value at -70hPa to allow for the comparison of electrode pairs and sample types. Finally, a nonlinear mixed-effects model with a log-log power-law form was used to describe the relationship between respiration flux and electrical conductivity, with random effects grouped by sample to account for heterogeneity among soil conditions.

3. Results

3.1. Soil respiration rates across soil matric potential and organic matter quantification

360 The organic matter content across the treatments showed no statistical difference ($F_{Welch}(7, 10.4) = 1.96, P = 0.16$), with a small to moderate effect size ($\omega_p^2 = 0.27, 95\% CI [0.00, 1.00]$). The lowest organic matter content was observed for the sieved topsoil conventional tillage samples and the highest amount was observed in the sieved conventional tillage subsoil (Fig. S3). At the highest saturation level, there was a significant increase in total respiration rate between the sieved compared to the undisturbed samples ($P < 0.03$) and the topsoil compared to the subsoil samples ($P < 0.002$) (Table S2). Organic matter (OM) content varied among individual soil samples (Fig. S3), ranging from approximately 3.6% to 14.1% of dry soil mass. The lowest OM content was observed in the sieved CT topsoil, whereas the highest values occurred in the undisturbed CT subsoil samples. However, OM content did not differ significantly among groups ($F_{Statistic(7, 10.4)} = 1.96, p = 0.16$). Aere weret the highest saturation level, a significant increasedifference in total respiration rate was observed between sieved and undisturbed samples ($p < 0.03$), as well as between topsoil and subsoil samples ($p < 0.002$) (Table S2).

370 The relative respiration rate, normalized to the values measured at -70 hPa, increased by approximately three orders of magnitude as pressure head increased (i.e., became less negative) from -996 to -70 hPa (Fig. 1). For the sieved samples, this trend was maintained across all pressure heads, with a small respiration peak observed at -100 hPa. In contrast, the undisturbed samples exhibited a respiration peak at -250 hPa. This increase was particularly pronounced for the topsoil conservation agriculture (CA) sample.

Mis en forme : Couleur de police : Texte 1

Mis en forme : Police :Couleur de police : Texte 1, Non Exposant/ Indice

Mis en forme : Police :Couleur de police : Texte 1

Mis en forme : Police :Couleur de police : Texte 1, Indice

Mis en forme : Police :Couleur de police : Texte 1, Indice

Mis en forme : Couleur de police : Accent 4

Mis en forme : Couleur de police : Accent 4

Mis en forme : Police :Italique

Mis en forme : Police :Italique, Indice

Mis en forme : Police :Italique

Mis en forme : Police :Italique

Mis en forme : Police :Italique, Couleur de police : Texte 1

375 Apart from this peak in the undisturbed samples, no significant differences were observed between sampling depths (topsoil versus subsoil) or field treatments (CT versus CA). Linear mixed-effects modelling indicated a significant effect of pressure head on respiration flux ($p = 0.0008$), but no significant effects of sample structure ($p = 0.178$), field treatment ($p = 0.436$), or their interactions.

380 In addition, no significant difference in relative respiration flux was detected between -996 and -630 hPa ($p > 0.618$). Post hoc comparisons further confirmed that relative respiration flux did not differ significantly among pressure heads beyond -450 hPa ($p = 0.311$). The relative respiration rate, normalised to the measured values at -70 hPa, showed a near consistent decrease across the tested matric potentials (Fig. 1). For the sieved samples, this decrease was maintained across all matric potentials, while for the undisturbed samples there was a respiration peak at -250 hPa. This increase was especially prominent for the topsoil conservation agriculture sample. Apart from the undisturbed sample values at this matric potential, no significant difference between sampling depth and field treatments was recorded. This was supported by the linear mixed-effects model

390 results (REML, Satterthwaite's method), which showed a significant effect of applied matric potential on respiration flux ($P = 0.0008$), but no significant effect of sample type ($P = 0.178$), field treatment ($P = 0.436$), or their interactions. Additionally, it should be mentioned that no significant difference in the relative respiration flux at -996 hPa and at -630 hPa was found ($P > 0.618$; Type III ANOVA, Satterthwaite's method). This finding was further supported by post hoc analysis confirming no significant difference after -450 hPa ($P = 0.311$; estimate marginal means with Kenward-Roger degrees of freedom).

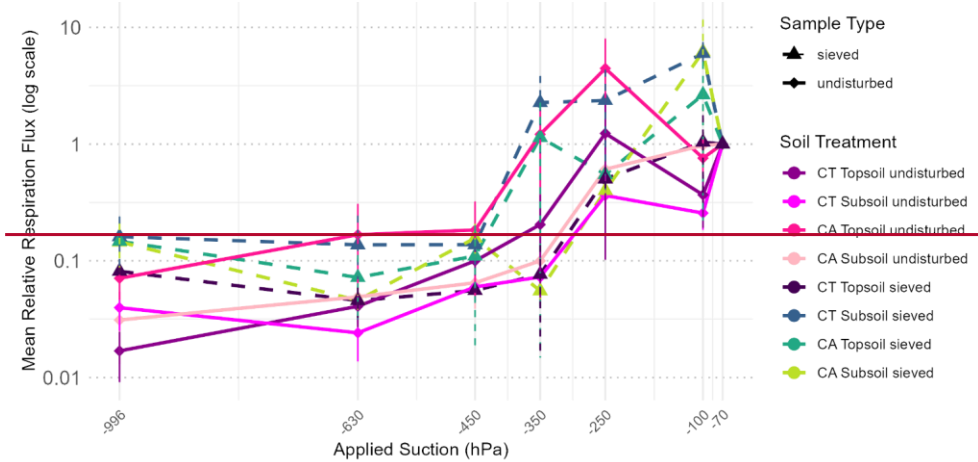
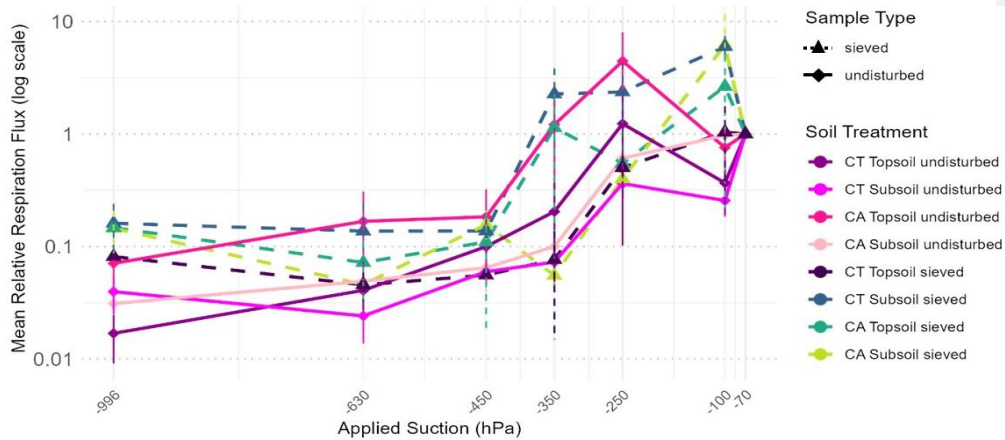
Mis en forme : Police :Italique

Mis en forme : Police :Italique

Mis en forme : Police :Italique

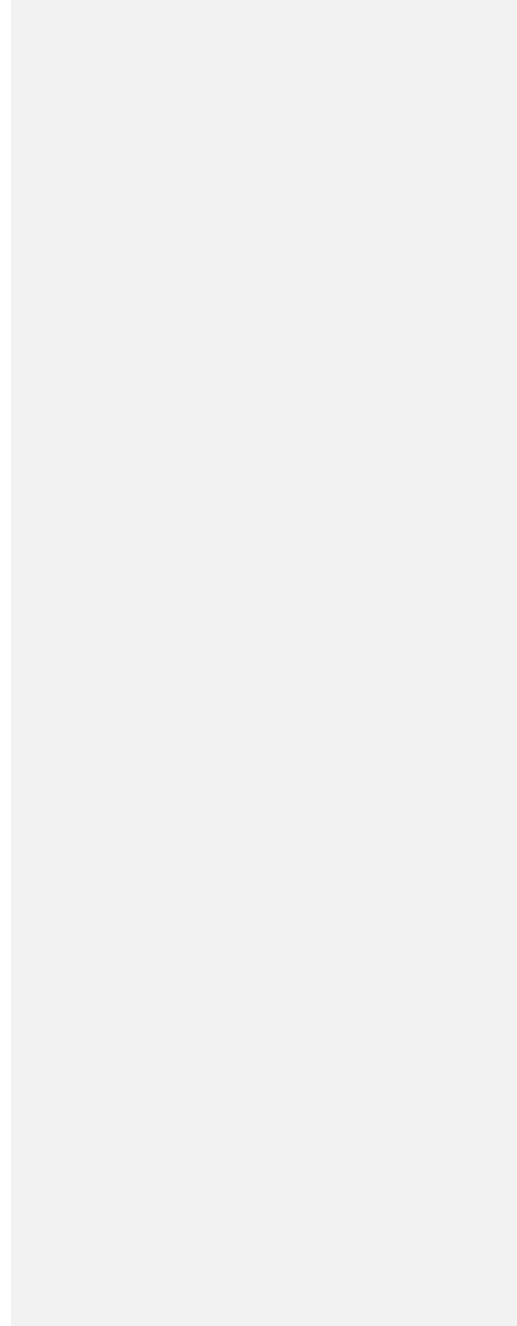
Mis en forme : Police :Italique, Couleur de police : Texte 1

Mis en forme : Police :Italique



395 Figure 1: Mean relative soil respiration flux obtained from the triplicate of each treatment measured at a range of different Applied
 Suctions (hPa). The different ~~suctions represent different soil matric potentials analysed over the course of~~ suction levels represent
 soil matric potentials analysed throughout the study. The sample abbreviation CA stands for conservation agriculture field
 400 treatment and CT stands for conventional tillage. The solid lines represent undisturbed soil cores while the dashed line corresponds
 to sieved samples. The relative respiration rate is normalised to the respiration rate observed at -70 hPa ~~corresponding to our highest
 tested saturation and are, corresponding to our highest tested saturation, and is~~ represented in a log scale. The error bars exceeding
 the marker size point are shown. For more details on averages and standard deviation of the mean, please consult Table S3 of our
 supplementary materials.

|



405 **3.2. Soil electrical conductivity across soil matric potential/water content**

Electrical conductivity (EC) measurements did not differ significantly between electrode channels within samples. Higher values were observed in the sieved conventional tillage (CT) topsoil ($1052 \mu\text{S cm}^{-1}$) and subsoil ($742 \mu\text{S cm}^{-1}$). Results for the conventional tillage (CT) samples are shown in Fig. 2, while the corresponding results for CA soils are provided in Fig. S5 of the Supplementary Material.

410 Across both CT and conservation agriculture (CA) systems, EC increased systematically with increasing water saturation (Fig. 2; Fig. S5). Although variability among individual cores was observed, no consistent separation between undisturbed and sieved treatments was evident across the full saturation range. Likewise, differences between topsoil and subsoil samples were not systematic. Two-way ANOVA applied to the fitted Archie saturation exponent (p , log-transformed) confirmed the absence of significant effects of depth, soil structure, or their interaction in either system (CT: depth $p = 0.72$, structure $p = 0.26$, interaction $p = 0.68$; CA: depth $p = 0.89$, structure $p = 0.77$, interaction $p = 0.90$).

415 In the undisturbed CT treatment, one replicate in both topsoil and subsoil showed a steeper decline in EC with decreasing water saturation (Fig. 2), leading to greater variability in the fitted EC- S_w relationships. This pattern was not observed in the CA samples or in other depth-structure combinations.

420 The EC-derived tortuosity factor (τ_w) increased with decreasing water saturation for all samples (Fig. 2; Fig. S5), reflecting progressively reduced diffusive transport at lower saturation levels. Although undisturbed samples exhibited greater variability across the saturation range, a two-way ANOVA applied to log-transformed τ_w revealed no significant effects of depth, soil structure, or their interaction in either management system (CT: depth $p = 0.57$, structure $p = 0.22$, interaction $p = 0.55$; CA: depth $p = 0.62$, structure $p = 0.56$, interaction $p = 0.64$). Similar results were obtained when τ_w values derived from the fitted curves were compared at $S_w = 0.3, 0.5$, and 0.8 for both management systems. Tereof the EC measurements across the soils analysed in the following only samples, is

425 T in ECN, due to the high variability among replicates no significant saturation were found
430 in de lower

Mis en forme : Titre 2

Mis en forme : Taquets de tabulation : 15,47 cm,Gauche

Mis en forme : Couleur de police : Texte 1

Mis en forme : Police :Italique

Mis en forme : Police :Italique

Mis en forme : Police :Italique

Mis en forme : Police :Italique

Mis en forme : Police :Italique

Mis en forme : Police :Italique

Mis en forme : Police :Italique

Mis en forme : Indice

Mis en forme : Police :Italique

Mis en forme : Indice

Mis en forme : Police :Italique

Mis en forme : Indice

Mis en forme : Police :Italique

Mis en forme : Police :Italique

Mis en forme : Police :Italique

Mis en forme : Police :Italique

Mis en forme : Police :Italique

Mis en forme : Police :Italique

Mis en forme : Indice

Mis en forme : Indice

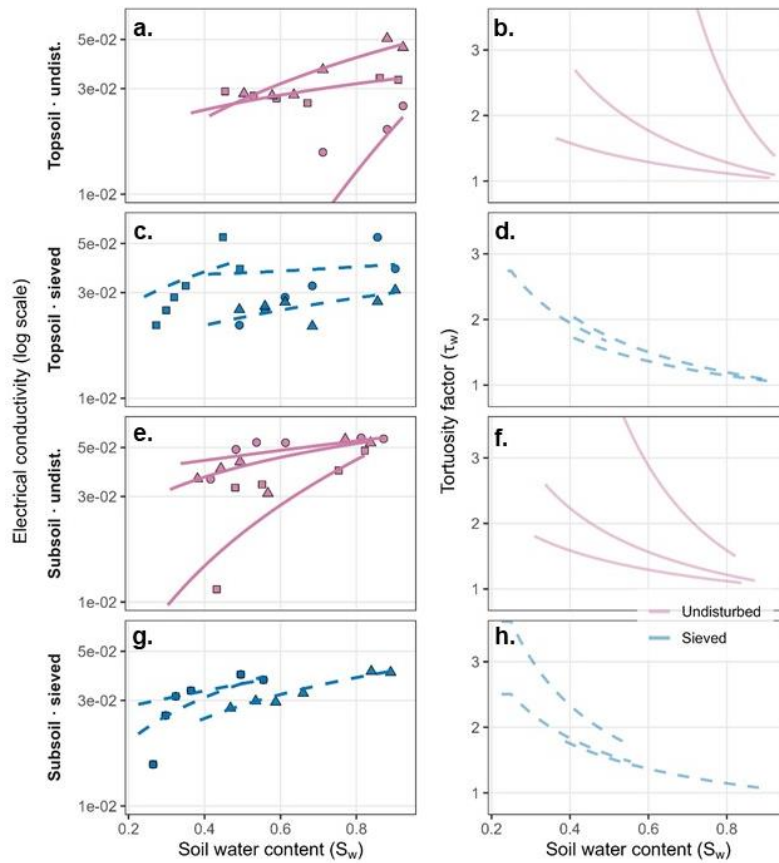


Figure 2: Electrical conductivity and derived tortuosity as a function of water saturation for soils under conventional tillage (CT) and conservation agriculture (CA).

(a, c, e, g) Bulk electrical conductivity (EC) plotted against water saturation (S_w) for topsoil and subsoil samples under undisturbed and sieved conditions. EC is shown on a logarithmic scale. Points represent measured values for individual soil cores, while lines represent fits of the pedophysical model (Eq. 4) applied separately to each core. Variability among individual cores resulted in differences in model fit quality for some samples.

Mis en forme : Indice

(b, d, f, h) Corresponding tortuosity factor (τ_w) derived from EC measurements using Eq. 5. Solid lines indicate undisturbed soils

Figure 2: Mean relative electrical conductivity

($n=3$), normalised to the rate observed at -70 hPa, is shown for the sieved samples (dashed line) and undisturbed (solid line) for the two different sample depths of the two field treatment types across a range of applied suctions (hPa). The applied suctions correspond to the associated soil matric potentials. The field treatment abbreviation CA stands for conservation tillage, while CT stands for conventional tillage. The averages are composed of three measurements of a triplicate of each Treatment type at each Applied Suction. The included standard deviation is not visible given its size did not exceed the size of the symbols. For more information on the associated averages and standard deviations of the means please consult Table S4-Table S8 of the supplementary materials.

440 and dashed lines indicate sieved soils. Model parameter estimates are provided in Table S5. The full dataset and corresponding fitted curves for all samples are provided in the Supplementary Material.

(a, c, e, g) the pedophysical relationship (Eq. 4) sample (b, d, f, h) inferred from EC measurements (Eq. 5).

445 There was a difference in pore water electrical conductivity (supplementary materials, Table S1) with most values ranging between 413 and 637 $\mu\text{S}/\text{cm}$, with the exception of the sieved conventional tillage top and subsoil which had values of 1052 and 742 $\mu\text{S}/\text{cm}$, respectively. To allow an easier comparison between samples given these differences, we chose to use the relative conductivity of each sampling depth and field trial to improve the comparability between samples.

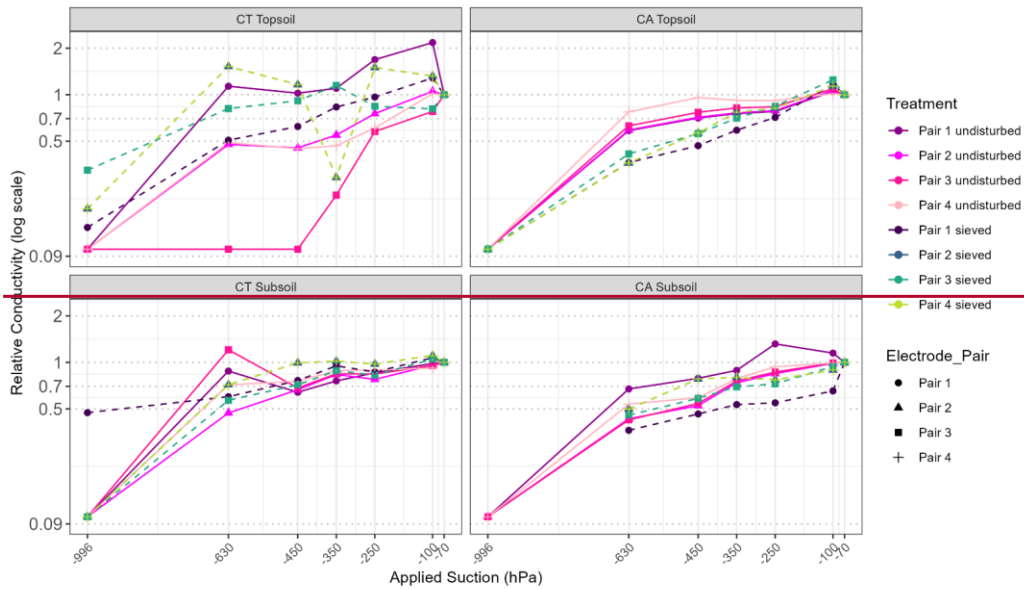
450 The majority of the electrode pairs show a consistent decrease as the matric potential decreased (Fig. 2). Exceptions to this relationship were recorded for the conventional tillage subsurface samples at -630 hPa for the electrode pairs 1 and 3 of the sieved samples and electrode pair 4 of the undisturbed samples. The measurements at -996 hPa for the sieved conventional tillage subsoil samples did not work and these results are excluded from our principal analysis. (Full range in Supplementary, Fig. S4) For the conventional tillage topsoil samples, the electrode pair 4 showed a high fluctuation across the measured matric potentials, as well as some small increases between -70 and -100 hPa. However, these were not statistically significant ($P=0.9703$). Finally, electrode pair 2 of the sieved conservation agriculture samples decreased more steeply than the other measurements. Besides these fluctuations, no difference between sampling depths nor differences between sieved and undisturbed samples were observed ($P=0.7$). For the conventional tillage topsoil samples, the electrode pair 4 showed a high fluctuation across the measured matric potentials, as well as some small increases between -70 and -100 hPa. However, these were not statistically significant ($P=0.9703$). Finally, electrode pair 2 of the sieved conservation agriculture samples decreased more steeply than the other measurements. Besides these fluctuations, no difference between sampling depths nor differences between sieved and undisturbed samples were observed ($P=0.7$);

Mis en forme : Indice

Mis en forme : Normal

Mis en forme : Police :9 pt, Gras, Surlignage

Mis en forme : Normal



3.3. Relationship between respiration flux and tortuosity factor Relationship between relative respiration rate and relative electrical conductivity

To evaluate whether respiration flux was coupled to diffusive transport constraints, linear regressions were fitted on \log_{10} -transformed respiration flux and \log_{10} -transformed EC-derived tortuosity variables related to (τ_w) for both CT and CA samples (Fig. 3, Fig. S6 for CA).

In the CT samples, respiration flux was negatively related to τ_w . Linear regressions were fitted using individual measurements from each soil core across the range of water saturations. A linear model including depth and structure confirmed a significant interaction between τ_w and soil structure ($p < 0.001$), indicating that slopes differed between undisturbed and sieved samples.

No significant interaction with depth was observed. Slopes and coefficients of determination for each depth-structure combination are summarised in Table S6.

In the CA samples, a significant overall negative relationship between respiration flux and τ_w was also observed ($F_{statistic(1, 58)} = 5.08, p = 0.028$). However, neither depth ($p = 0.90$) nor soil structure ($p = 0.72$), nor their interactions with τ_w significantly influenced the slope of the relationship. These results indicate that respiration decreased with increasing tortuosity in both management systems, although structural effects were only detectable in the CT samples.

Mis en forme : Police :Italique

Mis en forme : Police :Italique

Mis en forme : Indice

Mis en forme : Indice

Mis en forme : Justifié

Mis en forme : Police :Italique

Mis en forme : Police :Italique

Mis en forme : Police :Italique

Mis en forme : Indice

respirationtortuosity

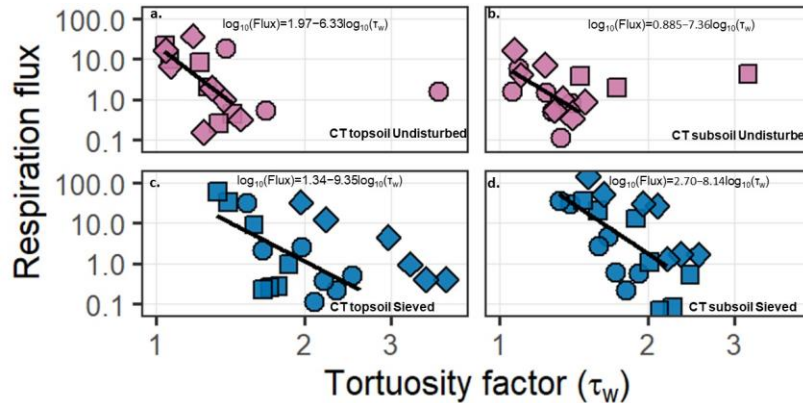


Fig. 3: Relationship between soil respiration flux and EC-derived tortuosity (τ_w) for the conventional tillage (CT) samples. Panels (a-b) show undisturbed samples and panels (c-d) show sieved samples. The left column corresponds to topsoil and the right column to subsoil. Points represent individual measurements from soil cores, with symbol shape indicating replicate. Respiration flux is plotted on a logarithmic scale. Solid black lines represent linear regressions fitted between log10-transformed respiration flux and log10-transformed tortuosity (τ_w) within the diffusion-limited range used for the statistical analysis. Only measurements within this range were included in the regressions. Regression equations are shown in each panel.

Log-log rR

The relationships between respiration rates and electrical conductivity were established after excluding the data at matric potentials above -250hPa because respiration rates in the undisturbed samples decreased between -250 and -70hPa (Fig. 1). This increase has been recorded in past studies and is caused by limitations in oxygen availabilities rather than substrate access (Moyano et al., 2013). Additionally, for improved visualization we selected to present only the electrode pairs 1 and 2. However, the entire data range is presented in the supplementary material (Supplementary Fig. S5).

Our results showed a decrease in the respiration and electrical conductivity with a decrease in soil matric potential which resulted in non-linear relationships between the two over the range of matric potentials studied (Fig. 3). Generally, the slopes of the relationships between the relative respiration rates and electrical conductivity revealed a steeper slope for the undisturbed samples compared to the sieved samples. The relationships were all statistically significant ($P < 0.02$), with the exception of the undisturbed conventional tillage top- and subsoil and sieved conservation agriculture subsoil measurements ($P > 0.1$). The R^2 values across treatments ranged from 0.07 to 0.84, with stronger relationships observed for undisturbed samples (e.g., CT

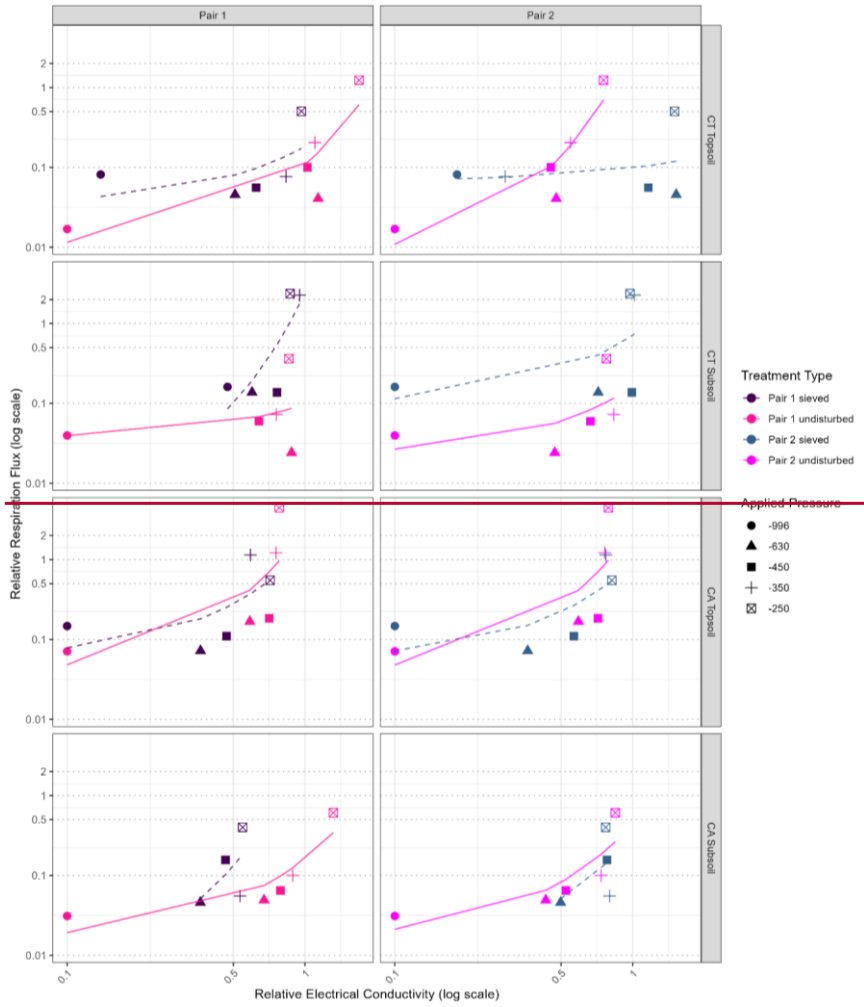
Mis en forme : Indice

Mis en forme : Indice

Mis en forme : Police :9 pt, Gras

Mis en forme : Normal

500 topsoil $R^2 = 0.84$, $P = 0.028$) and weaker or nonsignificant relationships for sieved samples (e.g., CA subsoil $R^2 = 0.28$, $P = 0.474$) (Table S9). Comparison of nested nonlinear mixed-effects models showed a statistically significant effect of the soil matric potential was found to be statistically significant ($P = 3.14 \times 10^{-16}$) supporting a strong effect of the water content on the soil respiration flux and electrical conductivity rate.



505 ~~Figure 3: Mean relative respiration flux (n=3) in relation to the mean relative electrical conductivity, normalised to the rate observed at the value observed at -70 hPa, is shown for the sieved samples (dashed line) and undisturbed (solid line) for the two sample depths of the two different field treatments across a range of applied suctions (hPa) illustrated by different marker points for the electrode pair 1 and 2. The average respiration was calculated based on triplicate respiration flux measurements of each treatment and the electrical conductivity represents the average of three measurements of each triplicates of each treatment at each applied suction. Additional information on the average respiration and average electrical conductivity as well as their associated standard deviations are presented graphically in Fig. 1 and Fig. 2 and in the supplementary materials in Table S2 and Table S3. The relationship between the two parameters is visualized in the form of an exponential model. The field treatment abbreviation CA stands for conservation tillage, while CT stands for conventional tillage. The measurements at -996 hPa for CA Subsoil has been excluded. Note that both axes have log scales.~~

515 4. Discussion

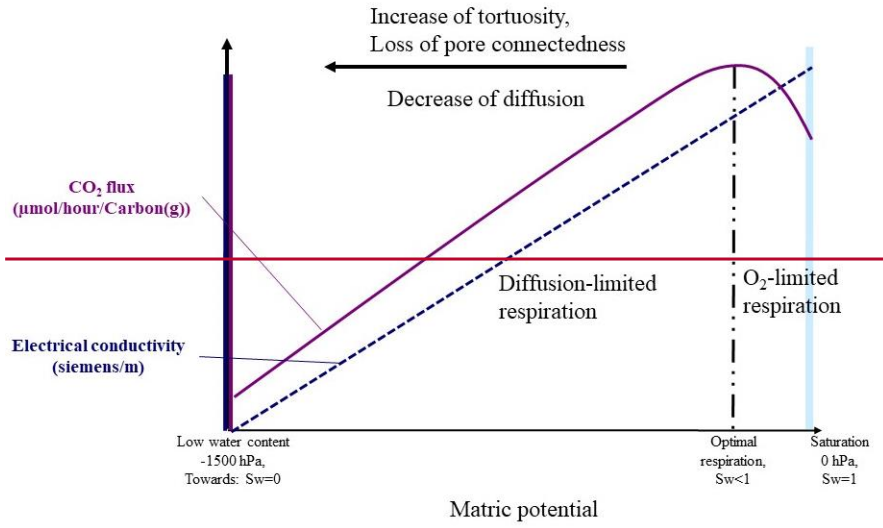
4.1. Electrical conductivity as a proxy of soil respiration

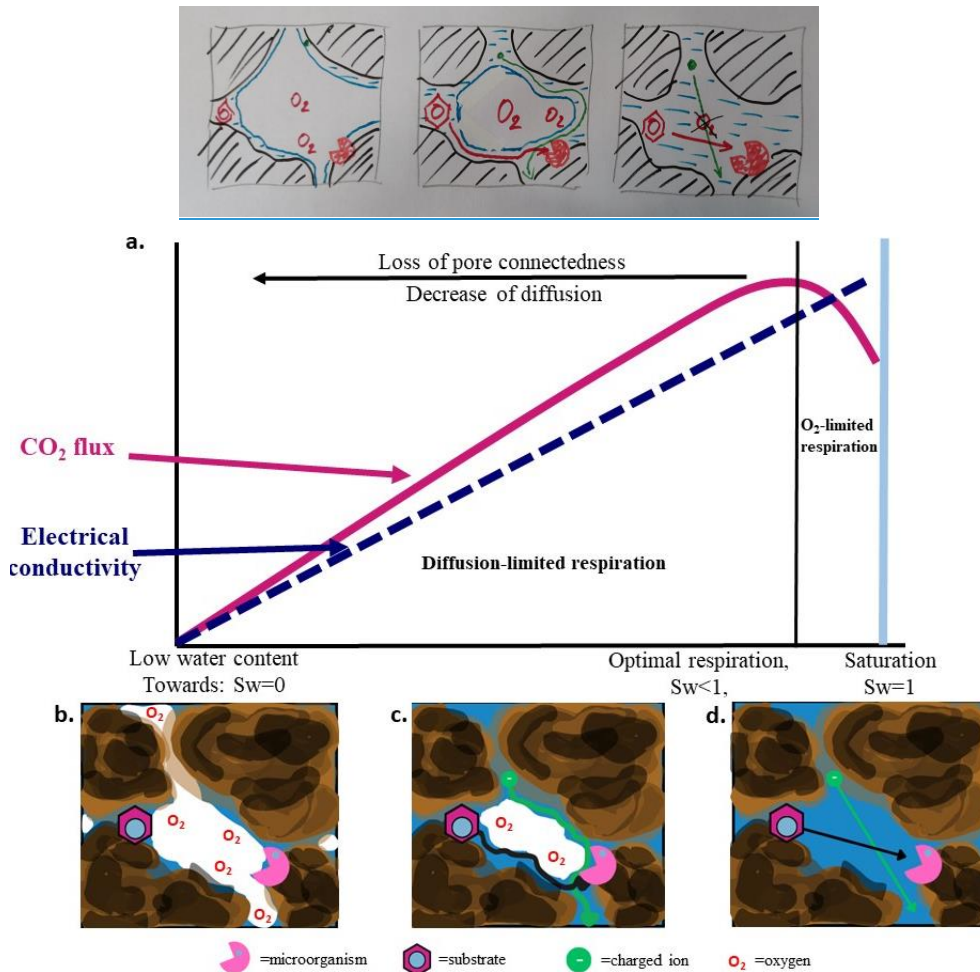
520 ~~We hypothesised that decreasing matric potential would be associated with reductions in both CO₂ flux and EC, reflecting reduced aqueous phase connectivity within the pore network (Fig. 3). Reduced water availability is known to increase hydraulic and electrical tortuosity, thereby constraining diffusive transport. We hypothesised that as matric potential decreases, CO₂ flux and electrical conductivity would decrease due to reduced pore connectivity of the aqueous phase in the pore network of the samples (Fig. 4). This loss of water availability increases hydraulic and electrical tortuosity, leading to a reduction in diffusion rates (Ghanbarian et al., 2013; Revil & Jougnot, 2008). Consistent with this conceptual framework, summarised in Fig. 4, both EC and soil respiration decreased as the soils dried. These declines were accompanied by an increase in τ_w with decreasing water saturation (Fig. 2).~~

525 ~~tend to. Our results tend to confirm this hypothesis, showing a decrease in both measured parameters as the soils dry, associated with a higher applied matric potential.~~

Mis en forme : Police :Italique

Mis en forme : Indice





530 **Figure 4: Conceptual framework linking soil respiration and electrical conductivity to water saturation. (a) Schematic**
 535 **representation of soil respiration (CO_2 flux) and bulk electrical conductivity (EC) as a function of water saturation (S_w). As**
saturation decreases from near saturation ($S_w = 1$) toward lower water contents, EC declines approximately monotonically due to
reduced pore-water connectivity. In contrast, respiration shows a non-linear response: at high saturation, respiration is limited by
oxygen diffusion; at intermediate saturation, respiration is maximized where oxygen supply and substrate connectivity are balanced;
and at low saturation, respiration becomes diffusion-limited due to reduced aqueous connectivity and restricted solute transport.

Mis en forme : Indice

Mis en forme : Indice

(b-d) Conceptual pore-scale illustrations corresponding to low water content (b), intermediate (optimal) saturation (c), and near-saturated conditions (d). The schematics show changes in microorganism–substrate–oxygen interactions and conductive pathways along the saturation gradient. Symbols represent microorganisms, substrates, charged ions, and oxygen as indicated.

540 Respiration peaked at -250 hPa in the undisturbed samples and did not increase further at higher saturation levels. Because respiration near saturation may reflect oxygen limitation rather than substrate diffusion, the highest saturation levels were excluded from the regression analyses linking respiration and tortuosity (Fig. 3). This plateau likely reflects reduced oxygen diffusion under near-saturated conditions, as oxygen diffuses more slowly through water than through air (Moyano et al., 2013). Only measurements within the diffusion-limited range below this peak were therefore included in the regression analyses, and this exclusion was applied consistently across structural treatments to ensure comparability.

545 Conceptual sketch of the links between respiration rate and electrical conductivity in soils associated with a decreasing saturation. The key difference between oxygen limited and diffusion limited respiration are indicated across the applied matric potentials.

550

Mis en forme : Interligne : 1,5 ligne

Mis en forme : Police :10 pt

Mis en forme : Normal (Web), Interligne : 1,5 ligne

555 An increase in respiration flux was observed at -250 hPa in the undisturbed samples. At higher saturation levels (-250 to 0 hPa in undisturbed samples and -100 to 0 hPa in sieved samples), respiration did not increase further. This plateau may reflect reduced oxygen diffusion under near-saturated conditions, as oxygen diffuses more slowly through water than through air

560 However, the undisturbed samples showed a respiration peak at -250 hPa while the sieved samples showed a small increase in respiration rate at -100 hPa (Fig. 1). This flux increase seen at -250 hPa is likely due to an optimal matric potential required for effective microbial carbon mineralisation first being reached at that potential. Above this optimal matric potential (i.e., -250 to 0 hPa for undisturbed and -100 to 0 hPa for sieved samples), the air phase is poorly connected in the soil porosity. As oxygen diffuses more slowly through water than air, microbial activity is likely limited, potentially leading to anoxic conditions at the microbial scale (Moyano et al., 2013). Similar non-monotonic responses of respiration to water content have been reported across soil types. This reduction in respiration at high saturation has been extensively documented across various soil types, supporting the validity of our measurements. It also highlights an optimal matric potential where oxygen availability and pore connectivity are balanced (Ebrahimi & Or, 2015; Moyano et al., 2013), suggesting the presence of a moisture range where oxygen supply and substrate diffusion are balanced.

565 Below this moisture range, respiration declined with decreasing water content. At lower saturation, reduced water availability increases tortuosity and constrained diffusive transport (Ebrahimi & Or, 2015; Ghezzehei et al., 2019). In this regime, EC and the derived tortuosity factor (τ_w) reflect changes in the geometry of the conductive phase and therefore provide information on conditions affecting diffusive transport (Revil & Jougnot, 2008; Jougnot et al., 2009).

570 A general decrease in EC with decreasing water saturation was observed in most samples (Fig. 2). This pattern is consistent with reduced connectivity of the water phase within the pore system, which increases electrical tortuosity and lengthens transport pathways

575 As the respiration rates close to saturation in the undisturbed samples were likely limited by oxygen availability up until -250 hPa rather than the diffusion of substrates, the measurements close to saturation were excluded for the comparison between relative respiration rates and relative electrical conductivity. For the sieved samples only a minor increase at -100 hPa was recorded, but for comparability the two highest saturations are also excluded of the correlation plots for our sieved samples (Fig. 3).

580 A general decrease in electrical conductivity with decreasing water saturation was observed in most samples, linked to a reduced connectivity of the water phase in the pore system (Fig. 2). This reduction in connected water phases yields an increase in electrical tortuosity (i.e., a proxy for diffusion tortuosity), lengthening the diffusion path of charge carrier ions until the water phase becomes disconnected (Ghanbarian et al., 2013; Jougnot et al., 2018). At sufficiently low saturation, the water phase approaches a percolation threshold where conductive pathways become increasingly disconnected (Hunt, 2005; Revil & Jougnot, 2008) until a percolation threshold under which the water phase becomes disconnected. Because solute and substrate diffusion occur primarily through the aqueous phase, this progressive loss of connectivity supports the interpretation that decreasing water saturation constrains microbial respiration through diffusion limitation (Hunt, 2005; Revil and Jougnot, 2008). In unsaturated porous materials;

Mis en forme : Police :Italique

590 Since ion movement depends on only occur in the water phase, quantity and it depends strongly on the water saturation and connectedness. However one has to keep in mind that but it is also influenced by the type of ions and electrical charges at the mineral surface (Revil & Jougnot, 2008). This concept of increased tortuosity is also further reflected in soil respiration in the form of the tortuosity of diffusion pathways of the substrates having to diffuse across a lengthened pathway to reach the microbial communities and thus consecutively decreasing at our highest tested matric potential.

595 Interestingly, at -630 hPa the second lowest water content in the conventional tillage subsoil samples, EC electrical conductivity showed an unexpected increase. A clear physical explanation is not evident; however, fungal growth was observed on the sample surface during the incubation period. Although speculative, fungal activity may have contributed to this isolated increase in EC. Fungal hyphae can modify their surrounding microenvironment through both chemical and physical processes, including mobilisation of phosphate ions and aggregate formation. While a clear physical explanation is lacking, we observed mould fungi on the sample surfaces between -250 and -350 hPa, suggesting a potential link. (Ameen et al., 2019; Hartmann & Six, 2022; Sun et al., 2022). Such local changes in pore-water chemistry or structure could influence measured conductivity. This feature was not observed in other depths or management systems, and therefore remains tentative.

600 Previous studies (Ameen et al., 2019; Sun et al., 2022) describe fungal-induced changes in microenvironment conductivity, possibly due to phosphate transformation or aggregate formation (Hartmann & Six, 2022). This feature was not observed for the other sampling depths and field treatments, suggesting that increased electrical conductivity could be linked to the presence of fungi. This assumption is supported by past studies describing physical and chemical changes in the microenvironment around fungal hyphae (Ameen et al., 2019; Sun et al., 2022). Regarding ionic changes in soil samples, these studies reported an increase in the conductivity of the microenvironment surrounding fungal hyphae, attributed to the transformation of phosphates from bound forms into free ions. In our study, this effect solely impacting the final pump measurement could be explained by the need for the fungal hyphae to have spread sufficiently between electrodes before their effect can be detected. Alternatively, fungi have been associated with aggregate growth and associated changes in porosity due to the clay particle encrusting of hyphae (Hartmann & Six, 2022). However, for the conservation tillage subsoil samples the electrical conductivity fell back down at -996 hPa which could mean that the loss of water content became too significant to maintain any increases associated with fungal presence.

615 In several cases, respiration did not differ significantly between the two lowest water saturations several cases the decrease in the respiration rate was not significant between -630 and -996 hPa (Fig. 1). This is consistent with reports of sigmoidal declines in respiration with decreasing water availability, where reductions may be gradual across specific matric potential ranges. These findings are supported by studies identifying a more sigmoidal decrease in respiration in relation to water availability meaning that between certain matric potentials the decrease will be more gradual (Curiel Yuste et al., 2007; Ghezzehei et al., 2019).

Mis en forme : Justifié

4.2. Impact of soil structure on the respiration-tortuosity relationship

The significant log-log relationship between respiration flux and EC-derived tortuosity (τ_w) observed within the diffusion-limited range (Fig. 3) indicates a coupling between microbial respiration and diffusive transport constraints. In the CT samples, steeper slopes were observed for sieved soils relative to undisturbed soils, suggesting that under homogenised structural conditions respiration responded more strongly to changes in tortuosity. This contrast was not evident in the CA samples.

We hypothesized that sieving would alter pore structure by producing a more homogeneous pore network, leading to a more uniform decline in EC and respiration compared to undisturbed samples. However, while sieving significantly affected respiration rates, this was not reflected in bulk EC values. Instead, the EC-derived tortuosity (τ_w) showed a more homogeneous response to water saturation in the sieved samples (Fig. 2d and h), consistent with a more uniform pore network following soil homogenisation. Respiration rates were also higher in sieved samples near saturation (Fig. 1).

We hypothesized that sieving would significantly impact our results by forming a more homogenous distribution of pore sizes in the pore network, leading to a more uniform decrease of the electrical conductivity and respiration rate compared to the undisturbed samples. However, while sieving did have a significant impact on the respiration rate, this was not values, but could be seen in the more homogeneous behavior of with water saturation (Fig. 2d and h) the case for the electrical conductivity values. In the case of soil respiration, the hourly flux of the sieved samples at saturation was significantly higher than that of the undisturbed samples (Fig. 1). Our findings align with a study by Herbst et al. (2016) who reported similar contrasts between sieved and undisturbed cores across a range of water contents.

comparing sieved and undisturbed soil cores across a broad water content range. Two mechanisms may explain the differences between sieved and undisturbed samples. Firstly, sieving alters pore size distribution, modifying hydraulic connectivity and drainage behaviour affecting the wetting process and allowing hydraulic pore connectivity to persist for longer (Castellini & Ventrella, 2012; Shaxson, 2006). Smaller and more uniformly distributed pores may retain water longer during drying, reinforcing contrasts between structural treatments at intermediate matric potentials. This change in pore structure could also help reduce nutrient leaching rate during the drying cycle, with smaller pore sizes taking longer to drain, thereby reinforcing the contrast between sieved and undisturbed samples at mid-range soil matric potential (Çelik et al., 2021; Gupta Choudhury et al., 2014).

Secondly, sieving can affect carbon availability to microbial decomposers. The physical protection of organic C from microbial decomposition is believed to be a major mechanism leading to organic C persisting in soil (Moyano et al., 2013; Six et al., 2006). Sieving may disrupt this protection by breaking aggregates and increasing contact between substrates and microbial communities. the physical protection, by breaking down soil aggregates and mixing, thus bringing organic substrate and microbial decomposers into close proximity, which is necessary for decomposition to occur. Improved aeration and substrate availability in sieved samples may therefore explain why soil respiration remains elevated even close to complete saturation.

The subsequent decline in respiration beyond the optimal matric potential further supports moisture limitation of decomposition. The steady decrease in respiration after reaching the optimal matric potential underlines that water availability

Mis en forme : Police :Italique

Mis en forme : Indice

Mis en forme : Police :Italique

Mis en forme : Indice

Mis en forme : Non Surlignage

is an important restricting factor for organic matter decomposition (Crawford, 2005; Fan et al., 2015). The absence of significant differences in EC between structural treatments indicates that sieving did not substantially alter bulk conductive properties. This difference in slopes indicates that soil structure influenced the sensitivity of respiration to tortuosity, even though τ_w itself did not differ significantly between structural treatments. Such decoupling between bulk physical transport metrics and biological response has previously been reported when bulk density and water content are comparable (Nadler, 1991).

The finding that there was no difference in relative electrical conductivities between sieved and undisturbed samples suggests that the difference in soil structure becomes the most evident for soil respiration while not being as important of an influence for the electrical conductivity effect of soils structural changes on. This finding can be explained by the fact that while particle shape and orientation are important factors influencing conductive pathway lengths, Nadler (1991) found that when bulk densities and water contents remain similar, the effect of particle size is negligible.

4.3. Impact of agricultural treatment

Although there were no significant differences in either relative respiration rate or relative electrical conductivity between the management systems, differences emerged in how respiration responded to changes in water availability and tortuosity. In particular, undisturbed topsoil samples from the CT system maintained comparatively higher respiration rates at higher matric potentials relative to the corresponding CA samples. Conventional tillage disrupts soil aggregates and redistributes organic matter within the plough layer, potentially enhancing substrate accessibility and microbial activity in topsoil horizons. Although there were no significant differences in either relative respiration rate or relative electrical conductivity between the field treatments, the relationships between the two differed significantly. The undisturbed conventional tillage samples exhibited a generally weaker correlation compared to the conservation agriculture samples, particularly for the topsoil samples caused by higher respiration rates still being maintained at higher matric potentials. These observations could be explained by past studies underlining conventional tillage promoting soil organic matter oxidation in the topsoil through the breakdown of large soil aggregates and consecutively distributing organic matter throughout the soil profile (Franco-Luesma et al., 2020; Zsolt et al., 2020). The stronger structural effects observed in the CT samples, particularly in the respiration- τ_w relationship, are consistent with this mechanism, as respiration in sieved CT soils responded more strongly to changes in tortuosity than in undisturbed soils (Fig. 3). In contrast, the absence of comparable structural modulation in the CA samples suggests that long-term aggregate stability may buffer respiration responses to changes in tortuosity.

In our measurements, this reasoning is further supported by this observed trend in the sieved samples being reversed, further underlining that breaking down big aggregates and consecutively mixing the liberated stored carbon across the samples can lead to higher respiration rates even at lower matric potentials.

4.4. Effects of topsoil compared to subsoil

685 Finally, we hypothesized that the relationships between respiration and electrical conductivity in the topsoil would not be as strong as the relationships in the subsoil due to the more ubiquitous distribution of OM across the pore system and therefore a reduced dependence on diffusion in the topsoil. However, no significant difference was found. We hypothesized that respiration-EC relationships would be weaker in the topsoil than in the subsoil due to a more homogeneous distribution of organic matter and therefore reduced diffusion dependence. However, no significant differences were detected. Because organic matter contents were similar between depths, substrate availability was likely comparable, and depth-related differences in diffusion dependence could not be resolved.

690 This does not mean that the hypothesis should be rejected, because the OM contents of the topsoil and subsoil were not significantly different either, suggesting that OM was equally available to decomposers in both. This means that the dependence of OM decomposition on diffusion as a function of OM availability could not be tested with these soils. Nevertheless, respiration rates in the topsoil were higher than in the subsoil at high moisture levels, indicating greater mineralisation potential under near-optimal conditions. The organic matter in the topsoil was significantly more mineralisable compared to the subsoil at higher moisture levels, which may be related to the nature of the OM. As the soils dried, the respiration rates in the topsoil and subsoil converged, suggesting that diffusion limitation increasingly constrained activity and masked depth-related differences. In sieved samples, this convergence between depths was less apparent, possibly because homogenisation reduced structural and substrate heterogeneity, thereby altering microbial access to organic matter. As the soils dried, the respiration rates in the topsoil and subsoil were similar, suggesting that the impact of the diffusion limitation became more limiting and masked any depth effect. This relationship between top and subsoil respiration rates is not maintained for the sieved soil samples. This discrepancy could be explained by the substrates being homogenized across the sample, which allowed better microbial access and, consequently, increased carbon mineralization (Salomé et al., 2010).

5. Conclusion

705 This study evaluated whether electrical conductivity (EC) measurements can serve as a proxy for soil respiration under diffusion-limited conditions, given the shared dependence of both processes on water-phase connectivity. Across soils differing in structure, depth, and management history, respiration decreased with declining water availability and increasing tortuosity. Log-log regressions revealed significant relationships between respiration flux and EC-derived tortuosity (τ_w), indicating that EC reflects transport constraints governing microbial activity. These findings suggest that EC provides quantitative information on diffusion-limited respiration in the absence of substantial advective water flow.

710 Structural treatments influenced the strength of the respiration- τ_w relationship, particularly in conventionally tilled soils, highlighting the role of pore-network organisation and substrate accessibility in modulating diffusion constraints.

Mis en forme : Police :Gras

Overall, the results support the interpretation that soil respiration is partly diffusion-limited under unsaturated conditions and that this limitation can be captured using EC-derived transport metrics. Future work should evaluate the robustness of this approach under field conditions and refine the quantitative framework linking EC-derived transport metrics to microbial process rates.

715

720 The present study investigated whether electrical conductivity measurements in soils can be used as a proxy of soil respiration
quantification given the reliance of both parameters on the availability of a connected water phase. This investigation tested
both sieved and natural soils from two long-term agricultural study fields and two different depths. Throughout our experiment,
we applied different suctions before measuring the increase in CO₂ content over 72 hours, as well as the electrical conductivity.
725 The analysis of the relationship between the two variables revealed a strong relationship across the tested soil matric potentials
confirming a similar effect in both parameters with loss of water availability. This leads us to conclude that electrical
conductivity could be used as a proxy to measure diffusion-limited microbial activity in the form of soil respiration rates.
Additionally, we observed a difference between the sieved and undisturbed samples showing an overall steeper decrease in
the undisturbed samples compared to the sieved ones. Our results are in support of the spatial distribution of organic matter
having a significant impact on soil respiration rates, therefore confirming that respiration in soils is, at least partly, diffusion-
limited in absence of significant water flow (i.e., rain events or important water table changes). This investigation tested both
sieved and natural soils from two long-term agricultural study fields and two different depths. Throughout our experiment, we
applied different suctions before measuring the increase in CO₂ content over 72 hours, as well as the EC. suggest

Mis en forme : Normal

730 This study paves the way to use electrical conductivity as a proxy for these diffusion processes though water connectedness
and tortuosity. Future works will be carried out to test this hypothesis further and provide a more quantitative framework to
mechanistically relate soil respiration and electrical conductivity in soils.

-Author contribution

735 The experimental conceptualization was a collaboration between all co-authors. Funding acquisition, project management and
supervision: DJ and NN; initial methodology development and validation: MG, OF; Investigation, Formal analysis: OF;
Visualization: OF, DJ, NN; Writing: First draft: OF; Rewriting and editing: NN, DJ, OF

Mis en forme : Normal

Competing interests

The authors declare that they have no conflict of interest.

740 Acknowledgements

The authors want to thank F. Delarue for his help with loss-on-ignition measurement.

Financial support

The PhD thesis O. Fülöp is supported by the BIOMASS project funded by the 80|PRIME program of the CNRS MITI.

References:

- 745 Allende-Montalbán, R., San-Juan-Heras, R., Martín-Lammerding, D., Delgado, M. D. M., Albarrán, M. D. M., & Gabriel, J. L. (2024). The soil sample conservation method and its potential impact on ammonium, nitrate and total mineral nitrogen measurements. *Geoderma*, *448*, 116963. <https://doi.org/10.1016/j.geoderma.2024.116963>
- Al-Maliki, S., & Ebreesum, H. (2020). Changes in soil carbon mineralization, soil microbes, roots density and soil structure following the application of the arbuscular mycorrhizal fungi and green algae in the arid saline soil. *Rhizosphere*, *14*, 100203. <https://doi.org/10.1016/j.rhisph.2020.100203>
- 750
- Ameen, F., AlYahya, S. A., AlNadhari, S., Alasmari, H., Alhoshani, F., & Wainwright, M. (2019). Phosphate solubilizing bacteria and fungi in desert soils: Species, limitations and mechanisms. *Archives of Agronomy and Soil Science*, *65*(10), 1446–1459. <https://doi.org/10.1080/03650340.2019.1566713>
- 755 Autret, B., Guillier, H., Pouteau, V., Mary, B., & Chenu, C. (2020). Similar specific mineralization rates of organic carbon and nitrogen in incubated soils under contrasted arable cropping systems. *Soil and Tillage Research*, *204*, 104712. <https://doi.org/10.1016/j.still.2020.104712>
- Autret, B., Mary, B., Chenu, C., Balabane, M., Girardin, C., Bertrand, M., Grandeau, G., & Beaudoin, N. (2016). Alternative arable cropping systems: A key to increase soil organic carbon storage? Results from a 16 year field experiment. *Agriculture, Ecosystems & Environment*, *232*, 150–164. <https://doi.org/10.1016/j.agee.2016.07.008>
- 760
- Bellone, D., Jeuffroy, M.-H., Bertrand, M., Mistou, M.-N., Barbu, C., Ballini, E., Morison-Valantin, M., Gauffreteau, A., & Pashalidou, F. G. (2023). Are innovative cropping systems less dependent on synthetic pesticides to treat Septoria leaf blotch (*Zymoseptoria tritici*) than conventional systems? *Crop Protection*, *170*, 106266. <https://doi.org/10.1016/j.cropro.2023.106266>
- 765

Blanchy, G., Deroo, W., De Swaef, T., Lootens, P., Quataert, P., Roldán-Ruíz, I., Versteeg, R., & Garré, S. (2025). Closing the phenotyping gap with non-invasive belowground field phenotyping. *SOIL*, *11*(1), 67–84. <https://doi.org/10.5194/soil-11-67-2025>

Castellini, M., & Ventrella, D. (2012). Impact of conventional and minimum tillage on soil hydraulic conductivity in typical cropping system in Southern Italy. *Soil and Tillage Research*, *124*, 47–56. <https://doi.org/10.1016/j.still.2012.04.008>

Çelik, İ., Günal, H., Acir, N., Barut, Z. B., & Budak, M. (2021). Soil quality assessment to compare tillage systems in Cukurova Plain, Turkey. *Soil and Tillage Research*, *208*, 104892. <https://doi.org/10.1016/j.still.2020.104892>

775 Chabert, A., & Sarthou, J.-P. (2020). Conservation agriculture as a promising trade-off between conventional and organic agriculture in bundling ecosystem services. *Agriculture, Ecosystems & Environment*, *292*, 106815. <https://doi.org/10.1016/j.agee.2019.106815>

Colas, E. (n.d.). *Impact de l'humidité et des solutions salines sur le comportement dimensionnel de grès du Buntsandstein :*

780 Cosentino, D., Chenu, C., & Le Bissonnais, Y. (2006). Aggregate stability and microbial community dynamics under drying–wetting cycles in a silt loam soil. *Soil Biology and Biochemistry*, *38*(8), 2053–2062. <https://doi.org/10.1016/j.soilbio.2005.12.022>

Crawford, R. L. (2005). Microbial Diversity and Its Relationship to Planetary Protection. *Applied and Environmental Microbiology*, *71*(8), 4163–4168. <https://doi.org/10.1128/AEM.71.8.4163-4168.2005>

785 Crowther, T. W., Van Den Hoogen, J., Wan, J., Mayes, M. A., Keiser, A. D., Mo, L., Averill, C., & Maynard, D. S. (2019). The global soil community and its influence on biogeochemistry. *Science*, *365*(6455), eaav0550. <https://doi.org/10.1126/science.aav0550>

- 790 Curiel Yuste, J., Baldocchi, D. D., Gershenson, A., Goldstein, A., Misson, L., & Wong, S. (2007). Microbial soil
respiration and its dependency on carbon inputs, soil temperature and moisture. *Global Change Biology*,
13(9), 2018–2035. <https://doi.org/10.1111/j.1365-2486.2007.01415.x>
- Davidson, Eric A., Belk, E., & Boone, R. D. (1998). Soil water content and temperature as independent or
confounded factors controlling soil respiration in a temperate mixed hardwood forest. *Global Change
Biology*, 4(2), 217–227. <https://doi.org/10.1046/j.1365-2486.1998.00128.x>
- 795 Dignac, M.-F., Derrien, D., Barré, P., Barot, S., Cécillon, L., Chenu, C., Chevallier, T., Freschet, G. T., Garnier,
P., Guenet, B., Hedde, M., Klumpp, K., Lashermes, G., Maron, P.-A., Nunan, N., Roumet, C., & Basile-
Doelsch, I. (2017). Increasing soil carbon storage: Mechanisms, effects of agricultural practices and
proxies. A review. *Agronomy for Sustainable Development*, 37(2), 14. <https://doi.org/10.1007/s13593-017-0421-2>
- 800 Dubey, R. K., Tripathi, V., Prabha, R., Chaurasia, R., Singh, D. P., Rao, Ch. S., El-Keblawy, A., & Abhilash, P.
C. (2020). *Unravelling the Soil Microbiome: Perspectives For Environmental Sustainability*. Springer
International Publishing. <https://doi.org/10.1007/978-3-030-15516-2>
- Ebrahimi, A., & Or, D. (2015). Hydration and diffusion processes shape microbial community organization and
function in model soil aggregates. *Water Resources Research*, 51(12), 9804–9827.
<https://doi.org/10.1002/2015WR017565>
- 805 Fan, L.-C., Yang, M.-Z., & Han, W.-Y. (2015). Soil Respiration under Different Land Uses in Eastern China.
PLOS ONE, 10(4), e0124198. <https://doi.org/10.1371/journal.pone.0124198>
- Franco-Luesma, S., Cavero, J., Plaza-Bonilla, D., Cantero-Martínez, C., Arrúe, J. L., & Álvaro-Fuentes, J.
(2020). Tillage and irrigation system effects on soil carbon dioxide (CO₂) and methane (CH₄) emissions
in a maize monoculture under Mediterranean conditions. *Soil and Tillage Research*, 196, 104488.
810 <https://doi.org/10.1016/j.still.2019.104488>

- Garre, S., Deswaef, T., Borra-Serrano, I., Lootens, P., & Blanchy, G. (2021). The potential of electrical imaging for field root zone phenotyping. *NSG2021 27th European Meeting of Environmental and Engineering Geophysics*, 1–5. <https://doi.org/10.3997/2214-4609.202120221>
- 815 Ghanbarian, B., Hunt, A. G., Ewing, R. P., & Sahimi, M. (2013). Tortuosity in Porous Media: A Critical Review. *Soil Science Society of America Journal*, 77(5), 1461–1477. <https://doi.org/10.2136/sssaj2012.0435>
- Ghezzehei, T. A., Sulman, B., Arnold, C. L., Bogie, N. A., & Berhe, A. A. (2019). On the role of soil water retention characteristic on aerobic microbial respiration. *Biogeosciences*, 16(6), 1187–1209. <https://doi.org/10.5194/bg-16-1187-2019>
- 820 Greenspan, L. (1977). Humidity fixed points of binary saturated aqueous solutions. *Journal of Research of the National Bureau of Standards Section A: Physics and Chemistry*, 81A(1), Article 1. <https://doi.org/10.6028/jres.081A.011>
- Gupta Choudhury, S., Srivastava, S., Singh, R., Chaudhari, S. K., Sharma, D. K., Singh, S. K., & Sarkar, D. (2014). Tillage and residue management effects on soil aggregation, organic carbon dynamics and yield attribute in rice–wheat cropping system under reclaimed sodic soil. *Soil and Tillage Research*, 136, 76–83. <https://doi.org/10.1016/j.still.2013.10.001>
- 825 Hargreaves, S. K., Williams, R. J., & Hofmockel, K. S. (2015). Environmental Filtering of Microbial Communities in Agricultural Soil Shifts with Crop Growth. *PLOS ONE*, 10(7), e0134345. <https://doi.org/10.1371/journal.pone.0134345>
- 830 Hartmann, M., & Six, J. (2022). Soil structure and microbiome functions in agroecosystems. *Nature Reviews Earth & Environment*, 4(1), 4–18. <https://doi.org/10.1038/s43017-022-00366-w>
- Henneron, L., Bernard, L., Hedde, M., Pelosi, C., Villenave, C., Chenu, C., Bertrand, M., Girardin, C., & Blanchart, E. (2015). Fourteen years of evidence for positive effects of conservation agriculture and

organic farming on soil life. *Agronomy for Sustainable Development*, 35(1), 169–181.

<https://doi.org/10.1007/s13593-014-0215-8>

835 Herbst, M., Tappe, W., Kummer, S., & Vereecken, H. (2016). The impact of sieving on heterotrophic respiration response to water content in loamy and sandy topsoils. *Geoderma*, 272, 73–82.

<https://doi.org/10.1016/j.geoderma.2016.03.002>

Hermans, T., Goderniaux, P., Jougnot, D., Fleckenstein, J. H., Brunner, P., Nguyen, F., Linde, N., Huisman, J.

A., Bour, O., Lopez Alvis, J., Hoffmann, R., Palacios, A., Cooke, A.-K., Pardo-Álvarez, Á., Blazevic, L.,

840 Pouladi, B., Haruzi, P., Fernandez Visentini, A., Nogueira, G. E. H., ... Le Borgne, T. (2023). Advancing measurements and representations of subsurface heterogeneity and dynamic processes: Towards 4D hydrogeology. *Hydrology and Earth System Sciences*, 27(1), 255–287. <https://doi.org/10.5194/hess-27-255-2023>

Hunt, A. G. (2005). Continuum percolation theory for transport properties in porous media. *Philosophical*

845 *Magazine*, 85(29), 3409–3434. <https://doi.org/10.1080/14786430500157094>

Jougnot, D., Jiménez-Martínez, J., Legendre, R., Le Borgne, T., Méheust, Y., & Linde, N. (2018). Impact of small-scale saline tracer heterogeneity on electrical resistivity monitoring in fully and partially saturated porous media: Insights from geoelectrical milli-fluidic experiments. *Advances in Water Resources*, 113, 295–309. <https://doi.org/10.1016/j.advwatres.2018.01.014>

850 Jougnot, D., Revil, A., & Leroy, P. (2009). Diffusion of ionic tracers in the Callovo-Oxfordian clay-rock using the Donnan equilibrium model and the formation factor. *Geochimica et Cosmochimica Acta*, 73(10), 2712–2726. <https://doi.org/10.1016/j.gca.2009.01.035>

Juarez, S., Nunan, N., Duday, A.-C., Pouteau, V., & Chenu, C. (2013). Soil carbon mineralisation responses to alterations of microbial diversity and soil structure. *Biology and Fertility of Soils*, 49(7), 939–948.

855 <https://doi.org/10.1007/s00374-013-0784-8>

- Kpemoua, T. P. I., Leclerc, S., Barré, P., Houot, S., Pouteau, V., Plessis, C., & Chenu, C. (2023). Are carbon-storing soils more sensitive to climate change? A laboratory evaluation for agricultural temperate soils. *Soil Biology and Biochemistry*, 183, 109043. <https://doi.org/10.1016/j.soilbio.2023.109043>
- Loiseau, B., Carrière, S. D., Jougnot, D., Singha, K., Mary, B., Delpierre, N., Guérin, R., & Martin-StPaul, N. K. (2023). The geophysical toolbox applied to forest ecosystems – A review. *Science of The Total Environment*, 899, 165503. <https://doi.org/10.1016/j.scitotenv.2023.165503>
- Lützw, M. V., Kögel-Knabner, I., Ekschmitt, K., Matzner, E., Guggenberger, G., Marschner, B., & Flessa, H. (2006). Stabilization of organic matter in temperate soils: Mechanisms and their relevance under different soil conditions – a review. *European Journal of Soil Science*, 57(4), 426–445. <https://doi.org/10.1111/j.1365-2389.2006.00809.x>
- Mondal, S., & Chakraborty, D. (2022). Global meta-analysis suggests that no-tillage favourably changes soil structure and porosity. *Geoderma*, 405, 115443. <https://doi.org/10.1016/j.geoderma.2021.115443>
- Moyano, F. E., Manzoni, S., & Chenu, C. (2013). Responses of soil heterotrophic respiration to moisture availability: An exploration of processes and models. *Soil Biology and Biochemistry*, 59, 72–85. <https://doi.org/10.1016/j.soilbio.2013.01.002>
- Nadler, A. (1991). EFFECT OF SOIL STRUCTURE ON BULK SOIL ELECTRICAL CONDUCTIVITY (ECa) USING THE TDR AND 4P TECHNIQUES. *152(3)*, 199–203.
- Nasiri, S., Andalibi, B., Tavakoli, A., Delavar, M. A., El-Keblawy, A., Zwieten, L. V., & Mastinu, A. (2023). The Mineral Biochar Alters the Biochemical and Microbial Properties of the Soil and the Grain Yield of *Hordeum vulgare* L. under Drought Stress. *Land*, 12(3), 559. <https://doi.org/10.3390/land12030559>
- Nunan, N., Schmidt, H., & Raynaud, X. (2020). *The ecology of heterogeneity: Soil bacterial communities and C dynamics*. *Philosophical Transactions of the Royal Society B*. <https://doi.org/10.1098/rstb.2019.0249>

- Poll, C., Pagel, H., Devers-Lamrani, M., Martin-Laurent, F., Ingwersen, J., Streck, T., & Kandeler, E. (2010). Regulation of bacterial and fungal MCPA degradation at the soil–litter interface. *Soil Biology and Biochemistry*, *42*(10), 1879–1887. <https://doi.org/10.1016/j.soilbio.2010.07.013>
- 880
- Ramonedá, J., Fan, K., Lucas, J. M., Chu, H., Bissett, A., Strickland, M. S., & Fierer, N. (2024). Ecological relevance of flagellar motility in soil bacterial communities. *The ISME Journal*, *18*(1), wrae067. <https://doi.org/10.1093/ismejo/wrae067>
- Revil, A., & Jougnot, D. (2008). Diffusion of ions in unsaturated porous materials. *Journal of Colloid and Interface Science*, *319*(1), 226–235. <https://doi.org/10.1016/j.jcis.2007.10.041>
- 885
- Salomé, C., Nunan, N., Pouteau, V., Lerch, T. Z., & Chenu, C. (2010). Carbon dynamics in topsoil and in subsoil may be controlled by different regulatory mechanisms: CARBON DYNAMICS IN TOPSOIL AND IN SUBSOIL. *Global Change Biology*, *16*(1), 416–426. <https://doi.org/10.1111/j.1365-2486.2009.01884.x>
- Shaxson, T. F. (2006). Re-thinking the conservation of carbon, water and soil: A different perspective. *Agronomy for Sustainable Development*, *26*(1), 9–19. <https://doi.org/10.1051/agro:2005054>
- 890
- Six, J., Frey, S. D., Thiet, R. K., & Batten, K. M. (2006). Bacterial and Fungal Contributions to Carbon Sequestration in Agroecosystems. *Soil Science Society of America Journal*, *70*(2), 555–569. <https://doi.org/10.2136/sssaj2004.0347>
- Stanford, G., & Smith, S. J. (n.d.). *Nitrogen Mineralization Potentials of Soils*. Soil Science Society of America Journal. Retrieved <https://doi.org/10.2136/sssaj1972.03615995003600030029x>
- 895
- Sun, R., Zhang, W., Liu, Y., Yun, W., Luo, B., Chai, R., Zhang, C., Xiang, X., & Su, X. (2022). Changes in phosphorus mobilization and community assembly of bacterial and fungal communities in rice rhizosphere under phosphate deficiency. *Frontiers in Microbiology*, *13*, 953340. <https://doi.org/10.3389/fmicb.2022.953340>

- 900 Van Genuchten, M. Th. (1980). A Closed-form Equation for Predicting the Hydraulic Conductivity of
Unsaturated Soils. *Soil Science Society of America Journal*, 44(5), 892–898.
<https://doi.org/10.2136/sssaj1980.03615995004400050002x>
- Waxman, M. H., & Smits, L. J. M. (1968). Electrical Conductivities in Oil-Bearing Shaly Sands. *Society of
Petroleum Engineers Journal*, 8(02), 107–122. <https://doi.org/10.2118/1863-A>
- 905 Zsolt, S., Tállai, M., Kincses, I., László, Z., Kátai, J., & Vágó, I. (2020). Effect of various soil cultivation
methods on some microbial soil properties. *DRC Sustainable Future: Journal of Environment,
Agriculture, and Energy*, 1(1), 14–20. <https://doi.org/10.37281/DRCSF/1.1.3>